Scientific
Research
Publishing

LiMnPO₄: Review on Synthesis and Electrochemical Properties

Joel O. Herrera[1*], Héctor Camacho-Montes[1], Luis E. Fuentes[2], Lorena Álvarez-Contreras[2]

[1]Universidad Autónoma de Ciudad Juárez, Cd. Juárez, México
[2]Centro de Investigación en Materiales Avanzados, Chihuahua, México
Email: [*]joel.obed.herrera@hotmail.com

Abstract

The olivine structured mixed lithium-transition metal phosphates LiMPO₄ (M = Fe, Mn, Co) have attracted tremendous attention of many research teams worldwide as a promising cathode material for lithium batteries and for studying their magnetic and electrical properties. High energy density is required for mind- to large-scale batteries because the mounting spaces are quite small for vehicles and other energy storage applications. This constraint necessitates synthesis to yield high volumetric energy density and reliable battery performance. Development of eco-friendly, low cost and high energy density, LiMnPO₄ cathode material became attractive due to its high operating voltage, which can be located inside of the electrochemical stability window of conventional electrolyte solutions and it offers more safety features due to the presence of a strong P-O covalent bond. This review is an overview of current research activities on LiMnPO₄ cathodes and its carbon coating synthesized by various synthetic techniques.

1. Introduction

Since the pioneering work of Goodenough *et al*. [1], the Phospho-olivine LiMPO₄ compound (with M equal Fe, Mn, Co or Ni) have been recognized as a potential positive electrode material for used in lithium rechargeable batteries. This family of materials has numerous advantages over the layered rock salt oxides (e.g. LiCoO₂ and LiNiO₂) that are currently used in commercial batteries. Besides its high discharge capacity ($\approx$170 mA·h·g⁻¹), LiMPO₄ cathode material shows high stability during lithium extraction/insertion and does not deteriorate when

---

[*]Corresponding author.

used at moderately high temperatures. Recently, a lot of effort has been devoted to optimize $LiFePO_4$ material. In particular, particle minimization with intimate carbon contact resulted in almost the theoretical capacity at moderate current densities with $LiFePO_4$ cathode material [2]. Surprisingly, only a few papers indicate the applicability of $LiMnPO_4$ [3]-[5] and, the results remain controversial.

The origin of the different electrochemical activities of isostructural $LiFePO_4$ and $LiMnPO_4$ is not quite clear at the moment. Yamada *et al.* [3] suggested that the low electrochemical activity of $LiMnPO_4$ is due to slow kinetics and internal friction during lithium extraction/insertion. Akin *et al*. has recently performed a comparative structural study [6] of these two materials and found minute differences in the oxygen vibrations in the Li layer. Yet another important factor is the magnetism in these compounds [7]-[9]. The magnetic properties are determined by the magnetic moment and may thus reflect the potential differences within the $LiMPO_4$ family. Magnetism is therefore indirectly important for electrochemical properties as well.

Figure 1 presents the schematics of the $LiMnPO_4$ olivine structure. $LiMnPO_4$ has an olivine structure, where Mn and Li occupy octahedral 4c and 4a sites, and P atom is in 4c site, respectively. The O atoms are in a hexagonal close-packed arrangement. The MnO_6 octahedral is separated by PO_4 plain that leads to the significant reduction of the electrical conductivity of the material. It results in a poor rate capability and a slow utilization of Li ions in the olivine host structure. Therefore, similarly to $LiFePO_4$, the successful preparation of high performance $LiMnPO_4$ could be achieved through the preparation of the conductive composites of fine particles of this material. However, the current durability of $LiMn_xPO_4$ is orders-of-magnitude inferior to that of Li_xFePO_4 [10], which make the preparation of the high conductivity $LiMnPO_4/C$ composites, more difficult than in the case of the lithium-iron phosphate.

In the olivine structures the magnetic ions occupy only the so-called M_2 site, *i.e.* the M_{2+} ion sits in the center of MO_6 unit. Each MO_6 distorted octahedron is connected to four other MO_6 via vertices forming a layered network perpendicular to the crystal (100) direction. Successive M_{2+} layers are separated by PO_4 tetrahedral and LiO_6 octahedral.

Only few routes synthesis for $LiMnPO_4$ has been proposed. Powder properties are strongly affected by the preparation technique. In this review, special attention is focused on obtaining $LiMnPO_4$.

2. Synthesis Method and Properties of LiMnPO₄

2.1. Solid-State Reaction

Some research groups have tried to use solid-state reactions to synthesize $LiMnPO_4$. The solid state reaction is a conventional synthesis method, which usually needs a two-step heating treatment, including the first firing in a temperature range of 300°C - 400°C and subsequent one between 600°C and 800°C. The solid state reaction method has been a developed technology and being used much frequently since it's simple to synthesis and easy to make mass production. The need for high temperature unfortunately upgrades cost; what is more, the product size always cannot be small. So other measures are added to circumvent those problems to process olivine
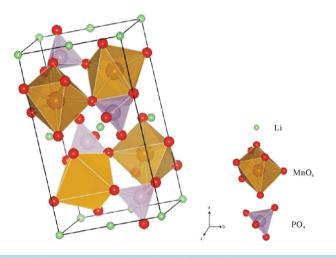

Figure 1. Structure of the $LiMnPO_4$ olivine with *Pnma* space group [10].

phosphates, such as slighter temperatures or adding carbon. **Table 1** shows the precursors used in the solid-state reaction of the resultant $LiMnPO_4$ and composites of this phase.

The effect of Fe_{+2} substitutions was successfully employed by Martha *et al.* [11] to form a solid solution between olivine phases of Fe and Mn. A solid state method was employed for the preparation of such a $LiMn_{0.8}Fe_{0.2}PO_4$ phase along with 10 wt% carbon by ball milling before the heat treatment at 550˚C for 3 h in Ar atm. The olivine phase $LiMn_{0.8}Fe_{0.2}PO_4$ comprised 25 - 60 nm size particulates with ≈5 nm thick carbon coating on the surface. Yang *et al.* [12] reported the synthesis of Co doped $LiMnPO_4$ ($LiMn_{0.95}Co_{0.5}PO_4$) by an oleic acid assisted approach. The source materials were initially ball milled before the heat treatment in N_2 atmosphere at various calcination temperatures.

The sample prepared at 600˚C performed better when compared to other temperature conditions and it showed discharge capacities of 103 and 144 mA·h·g^{-1} for $LiMnPO_4$ and $LiMn_{0.95}Co_{0.5}PO_4$ respectively at a 0.05 C rate between 2.5 and 4.5 V is using the CC-CV protocol. $LiMnPO_4$ with off-stoichiometry ($LiMn_{0.9}P_{0.95}O_{4-5}$) was reported by Kan and Ceder [13] with a particle size of <50 nm. The preparation phase contains some impurity phases like Li_3PO_4 and $Li_4P_2O_7$; the concentration of those phases was totally less than 5% of native compound, hence the theoretical capacity of $LiMnPO_4$ was assumed to be 162 mA·h·g^{-1}. To prepare Fe and Mg co-doped $LiMnPO_4$ with 14 wt% of sucrose, a solid-state route has been adopted with subsequent ball milling for 6 h by Hu *et al.* [14] [15]. Four different synthesis temperatures, namely, 650˚C, 750˚C, 800˚C and 850˚C were studied. When the temperature exceeds 800˚C it leads to the formation of Fe_2P impurity during Fe substitution. Hence, 800˚C for 10 h was well suited to obtain the best performing single phase material. The final comprised ≈ 7.5 wt% carbon for all the three temperatures except 850˚C (≈5.7 wt%). The electrochemical properties of $C-LiMn_{0.9}Fe_{0.1-x}Mg_xPO_4$ where x = 0.01, 0.02 and 0.05 were evaluated using CC-CV mode at 4.5 V vs Li.

Capacity profiles increased with increasing synthesis temperature and it could be attributed to the increased electronic conductivity of the carbon film. Hong *et al.* [16] reported Fe substituted olivine phase, $LiMn_{1-x}Fe_xPO_4$ (x = 0, 0.05, 0.1, 0.15. and 0.2) prepared with an appropriate amount of citric acid as the carbon source and subsequently employed planetary ball milling for about 3.5 days before the heat treatment. All the prepared showed similar diffraction patterns, except for a slight shift towards higher angles with increasing concentration of Fe ions and the unit cell shrank continuously as iron was introduced into the system. The cell experienced a discharge capacity of ≈133 and ≈138 mA·h·g^{-1} at 0.1 C between 2.8 and V by CC mode for 15 and 20% of Fe concentration, and those cells presented solid-solution behavior when the Fe concentration exceeds 10% when compared to the native compound (55 mA·g^{-1} at 0.067 C). Muraliganth and Manthiram [17] reported the solid-solution between $LiMnPO_4$ and either $LiCoPO_4$ or $LiFePO_4$ by a high energy ball milling procedure with 20% carbon in the final product. The discharge capacity increases significantly from 91 mA·h·g^{-1} in $LiMnPO_4$ to 142 mA·h·g^{-1} in $LiMn_{0.75}Fe_{0.25}PO_4$, and 155 mA·h·g^{-1} for $LiMn_{0.5}Fe_{0.5}PO_4$ at 0.05 C, whereas $LiCoPO_4$ and $LiMnPO_4$ solid solution experienced severe capacity fade due to the poor compatibility of the electrolyte.

2.2. Spray Pyrolysis.

Spray pyrolysis is an important method for the preparation of ultrafine powders [18] [19] and it is based on the generation of droplets in a continuous way from a solution containing precursor colloidal particles. Droplets can

Table 1. Precursors used in the solid state reaction method of the resulting powder.

Li Precursor	Mn Precursor	PO$_4$ Precursor	Metal Dopant	Carbon Source	Product	Discharge Capacity (mA·h/g)	Ref.
LiH_2PO_4	$MnCO_3$		$Fe(C_2O_4)\cdot2H_2O$	Carbon black	$LiMn_{0.8}Fe_{0.2}PO_4/C$		[11]
$LiOH\cdot H_2O$	Mn_2O_4	$(NH_4)_2PO_4$	Co_3O_4	Oleic acid.	$LiMn_{0.95}Co_{0.5}PO_4/C$		[12]
Li_2CO_3	$MnC_2O_4\cdot2H_2O$	$(NH_4)_2PO_4$			$LiMnPO_4$	103 - 144	[13]
LiH_2PO_4	$MnC_4H_6O_4\cdot4H_2O$		$Fe(C_2O_4)\cdot2H_2O$, $Mg(C_4H_6)\cdot4H_2O$	sucrose	$LiMn_{0.9}Fe_{0.1-x}Mg_xPO_4/C$	162	[14] [15]
Li_2CO_3	$MnCO_3$	$(NH_4)_2PO_4$	$Fe(C_2O_4)\cdot2H_2O$	Citric Acid	$LiMn_{1-x}Fe_xPO_4/C$	133 - 138	[16]
Li_2CO_3	$MnC_2O_4\cdot2H_2O$	$(NH_4)_2PO_4$	$Fe(C_2O_4)\cdot2H_2O$		$LiMn_{0.5}Fe_{0.5}PO_4$	91 - 142 - 155	[17]

be generated by using different techniques, such as ultrasonic transduction [20]. In spray pyrolysis, the generation of droplets is a key step because the droplets act as the nucleation centers and eventually evolve to well-crystallized, dense, and pure particles. **Table 2** shows the precursors used in the Spray Pyrolysis method of the resultant LiMnPO$_4$ and composites of this phase. The pyrolysis product is collected in a series of water bubblers at the reactor outlet where the salt by product dissolves leaving LiMnPO$_4$. In the recent past, Taniguchi and co-workers [21]-[26] reported the synthesis of LiMnPO$_4$ by spray pyrolysis followed by wet ball milling with 10% acetylene black and ethanol to make the carbon composite. Finally, the composite was fired at 500°C for 4 h in a N$_2$ + 3% H$_2$ environment and found that discharge capacity increases with the charge cut-off voltage. The influence of surface area on the electrochemical performance of LiMnPO$_4$ was also reported by the same authors by adjusting the firing temperature and increasing acetylene black concentration (20%). The solid solution between LiMnPO$_4$ and LiCoPO$_4$ was also reported by the same group using the spray pyrolysis technique [26]. The prepared LiCoxMnx^{-1}PO4 (x = 0, 0.2, 0.5, 0.8 and 1) powders were milled with 10% wt% acetylene black in ethanol by high energy ball-milling t form composites with carbon. The cells were tested at a 0.5 C rate and delivered an initial discharge capacity of 165 mA·h·g^{-1} at x = 0, 136 mA·h·g^{-1} at x = 0.2, 132 mA·h·g^{-1} at x= 0.5, 125 mA·g·h^{-1} at x = 0.8 and 132 mA·g·h^{-1} at x = 1.0, respectively.

Oh *et al.* [27]-[29] continued the work of ultrasonic spray pyrolysis initiated by Taniguchi and co-workers with spherical size LiMnPO$_4$ particulates. Carbon coating over the particulates was employed by mixing with sucrose, which was followed by ball milling at a speed of 100 rpm for 20 h and subsequently heat treated with different calcination temperatures (550°C, 650°C and 700°C in Ar-H$_2$ atm) ball milling followed by a sintering process led to the destruction of the spherical shape morphology and the final carbon content in the composite was found to be ≈3 wt%. It is obvious that increasing the calcination temperature results in an increase in crystallite size (52, 56 and 60 nm for 550°C, 650°C and 700°C) and decrease in specific surface area.

2.3. Co-Precipitation

This method needs a shorter reaction time and lower temperature compared with the solid state reaction. The particle size can reach the nanometer level and this reduced size can help to enhance the charge-discharge performance especially at big current condition. The inadequacies inhibiting the mass production are the complex process and large power consumption. **Table 3** shows the precursors used in the co-precipitation method of the

Table 2. Precursors used in the spray pyrolysis method of the resultant powders.

Li Precursor	Mn Precursor	PO$_4$ Precursor	Metal Dopant	Carbon Source	Product	Discharge Capacity (mA·h/g)	Ref.
LiNO$_3$	Mn(NO$_3$)$_2$·6H$_2$O	H$_3$PO$_4$		Acetylene Black	LiMnPO$_4$/C	165	[21]
LiNO$_3$	Mn(NO$_3$)$_2$·6H$_2$O	H$_3$PO$_4$		Acetylene	LiMnPO$_4$/C	136	[22]
LiNO$_3$	Mn(NO$_3$)$_2$·6H$_2$O	H$_3$PO$_4$		Acetylene Black	LiMnPO$_4$/C	132	[23]
LiNO$_3$	Mn(NO$_3$)$_2$·6H$_2$O	H$_3$PO$_4$			LiMnPO$_4$	125	[24]
LiNO$_3$	Mn(NO$_3$)$_2$·6H$_2$O	H$_3$PO$_4$			LiMnPO$_4$	132	[25]
LiNO$_3$	Mn(NO$_3$)$_2$·6H$_2$O	H$_3$PO$_4$		Carbon Black	LiMnPO$_4$/C	132	[26]
LiH$_2$PO$_4$	Mn(NO$_3$)$_2$·4H$_2$O		Fe(NO$_3$)$_3$·9H$_2$O		LiMn$_{1-x}$Fe$_x$PO$_4$		[27]
LiH$_2$PO$_4$	Mn(NO$_3$)$_2$·4H$_2$O				LiMnPO$_4$		[28]
LiH$_2$PO$_4$	Mn(NO$_3$)$_2$·4H$_2$O			Acetylene Black	LiMnPO$_4$/C		[29]

Table 3. Precursors used in the co-precipitation method of the resultant powders.

Li Precursor	Mn Precursor	PO$_4$ Precursor	Metal Dopant	Carbon Source	Product	Discharge Capacity (mA·h/g)	Ref.
LiCO$_3$	MnC$_2$O$_4$·2H$_2$O	NH$_4$H$_2$PO$_4$		Acetylene Black	Li$_x$MnPO$_4$/C		[30] [31]
LiH$_2$PO$_4$	Mn(CH$_3$CO$_2$)$_2$·4H$_2$O		Fe(CH$_3$CO$_2$)$_2$·4H$_2$O	Acetylene Black	LiMn$_{0.5}$Fe$_{0.5}$PO$_4$/C	75 - 110	[32]
LiH$_2$PO$_4$	Mn(CH$_3$CO$_2$)$_2$·4H$_2$O		Fe(CH$_3$CO$_2$)$_2$·4H$_2$O		LiMn$_{0.85}$Fe$_{0.15}$PO$_4$	125 - 140	[33] [34]

resultant $LiMnPO_4$ and composites of this phase. Non-stoichiometries proportions of lithium deficient ($Li_{0.5}MnPO_4$ and $Li_{0.8}MnO_4$) and rich phases ($Li_{1.1}MnPO_4$ and $Li_{1.2}MnPO_4$) were synthesized and reported by Xiao *et al.* [30] using co-precipitation followed by a solid-state approach with ball milling of carbon.

In all the non-stoichiometric compounds of Li_xMnPO_4 phases, traces of impurities like $Mn_2P_2O_7$ or Li_3PO_4 unavoidably co-existed with the native phase. The observed impurity phases were consistent with the phases observed in another olivine compound such as $LiFePO_4$ [30] [31]. The half-cells comprising $LiMnPO_4$, $Li_{1.1}MnPO_4$ and $Li_{1.2}MnPO_4$ phases displayed almost the same initial discharge capacity of ≈ 124 $mA \cdot h \cdot g^{-1}$ at 0.05 C rate between 2 and 4.5 V by CC-CV mode, whereas $Li_{0.5}MnPO_4$ and $Li_{0.8}MnO_4$ exhibited ≈ 75 and 110 $mA \cdot h \cdot g^{-1}$, respectively. Oh *et al.* [32] reported the reduction of polarization of the electrode and the least amount of Mn dissolution in $C\text{-}LiMn_{0.5}Fe_{0.5}PO_4$ by a precipitation technique. Initially, olivine $LiMn_{0.5}Fe_{0.5}PO_4$ was carbon coated with carbon (3.3 wt%) and it delivered a discharge capacity of ≈ 125 and ≈ 140 $mA \cdot h \cdot g^{-1}$ at 0.05 C rate at room temperature and 55°C, respectively, between 2.7 and 4.5 V vs Li by CC-CV mode. The same group reported the performance of micron-sized nanoporous $C\text{-}LiMn_{0.85}Fe_{0.15}PO_4$ with high volumetric capacity [33]. The capacity delivered by the micron-$LiMn_{0.85}Fe_{0.15}PO_4$ electrode was nearly 1.4 times higher than that of the nano-$LiMn_{0.85}Fe_{0.15}PO_4$ electrode, *i.e.*, 369.3 $mA \cdot h \cdot cm^{-3}$ versus 261.1 $mA \cdot h \cdot cm^{-3}$ under above test conditions. Double structured $LiMn_{0.85}Fe_{0.15}PO_4$ coordinated with $LiFePO_4$ was also reported by Oh *et al.* [34]. The core contained $LiMn_{0.85}Fe_{0.15}PO_4$ to enable high energy density and the outer layer was composed of $LiFePO_4$ to facilitate high rate capability. Carbon was also coated over the outer layer to increase the electronic conductivity.

2.4. Hydrothermal and Solvothermal Routes

Hydrothermal and solvothermal synthesis is a chemical process that occurs in an aqueous solution of mixed precursors above the boiling temperature of water and alcohol respectively. On these routes, it is possible to avoid the calculation step and obtain pure powders directly from the heated solution. However, if the carbon coating is desired, it is necessary to carry out the calcination step at high temperatures. During the synthesis, heated water or alcohol accelerates the diffusion of particles and the crystal growth is relatively fast. Both routes are typically carried out in a closed system called autoclave and there are less environmental concerns than many other powder production technologies.

Therefore, hydrothermal and solvothermal synthesis is a simple, clean and relatively low-cost methods that can be used to produce powders with high uniformity and purity [35]-[37]. **Table 4** shows the precursors used in the hydrothermal and solvothermal routes of the resultant $LiMnPO_4$ and composites of this phase. Fang *et al.* [38] [39] reported the successful preparation of $LiMnPO_4$ plates by a simple hydrothermal route in a basic medium at

Table 4. Precursors used in the hydrothermal and solvothermal routes of the resultant powders.

Li Precursor	M n Precursor	PO₄ Precursor	Metal Dopant	Carbon Source	Product	Discharge Capacity (mA·h/g)	Ref.
Li_2SO_4	$MnSO_4$	$NH_4H_2PO_4$			$LiMnPO_4$	68	[38] [39]
LiOH	$MnSO_4 \cdot H_2O$	H_3PO_4	$Mg(NO_3)_2 6H_2O$ $NiSO_4 \cdot 6H_2O$ $CuSO_4 \cdot 5H_2O$		$LiMn_{1-x}(Mg\ Ni\ Cu)_xPO_4$	107	[40]
$LiPO_4$	$MnPO_4$			Carbon black	$LiMnPO_4/C$	49 - 107	[41] [42]
LiH_2PO_4	$MnCO_3$		$FeC_2O_4 \cdot 2H_2O$	Acid lactone	$LiMn1_{1-x}Fe_xPO_4/C$	50 - 65	[43]
LiOH	$Mn(CH_3COO)_2 \cdot 4H_2O$	H_3PO_4		Multiwalled Carbon nanotubes (MWCNT)	$LiMnPO_4/MWCNT$		[44]-[46]
LiOH	$MnSO_4 \cdot H_2O$	H_3PO			$LiMnPO_4$		[47]
LiOH	$Mn(CH_3COO)_2 \cdot 4H_2O$	H_3PO_4	$CuSO_4 \cdot 5H_2O$		$LiMn_{0.98}Cu_{0.02}PO_4$ $LiMn_{0.95}Cu_{0.98}PO_4$	76 - 101 - 121	[48]
$LiOH \cdot H_2O$	$MnSO_4 \cdot H_2O$	H_3PO_4			$LiMnPO_4$	92 - 120 - 126 - 147	[49]
Li_3PO_4	$MnSO_4 \cdot 5H_2O$				$LiMnPO_4$	135	[50]

200˚C. The results clearly indicate that the prepared materials were in the nanometric range and actively participated in the electrochemical reaction in which plate-like $LiMnPO_4$ ball milled with 20% of carbon delivered a discharge capacity of 68 mA·h·g^{-1} between 3 and 4.5 V at 1.5 mA g^{-1}. Divalent cation doping (10%) such as Mg, Ni, Co, Zn, and Cu, was reported by Chen *et al*. [40] via a hydrothermal approach. The substitution of Mn sited leads to a decrease in lattice parameter values. The cell volume also decreased 0.8% for Mg_{2+}, 0.6% for Ni_{2+}, 0.3% for Cu_{2+}, and 0.4% for Zn_{2+} substitution consistent with their smaller ionic radii. A citric acid assisted facile one step solvothermal (equiv. volume mixture of water and ethanol) procedure was adopted by Wang *et al*. [41] [42] to synthesize the microspherical $LiMnPO_4$ at 300˚.

The obtained microspherical particles were mixed with glucose followed by heat treatment for carbon coating. The Li/$LiMnPO_4$ cell displayed a discharge a capacity of 107 mA·h·g^{-1} at 0.01 C with an appreciable plateau around ≈4.2 vs Li. As expected, increasing the current rate leads to poor cell performance; for example, at 1 C test cell presented a discharge capacity of 49 mA·h·g^{-1}. By introducing cetyltrimethylammonium bromide (CTAB) as a chelating agent in the above solvent mixture at relatively low temperature conditions (240˚C) $LiMnPO_4$ nanorods can be obtained. The storage performance of nanoplatelets of $LiMnPO_4$ and $LiFe_{0.5}Mn_{0.5}PO_4$ was studied by Saravanan *et al*. [43] using a simple solvothermal method at 250˚C for 8 h with gluconic acid p-lactone. The final $LiMnPO_4$ and Fe doped phases comprised of 10 wt% carbon. The test cells exhibited a discharge capacity of ≈50 and 65 mA·h·g^{-1} between 2.3 and 4.5 V by CC mode. Further, the same group of authors continued the work on solid-solutions of $LiMn_{11-x}Fe_xPO_4$ nanoplates by tuning various parameters, such as source materials, precursor concentration, effect of solvent, synthesis temperature and conducting coatings using the same approach. Manthiram and co-workers [44]-[46] reported a facile route to produce nanostructured $LiMnPO_4$ by a microwave assisted hydrothermal or solvothermal approach. In the hydrothermal approach, glucose is used as the source material for carbon, whereas MWCNTs were painted on the surface to enable a conducting network for $LiMnPO_4$ nanorods by the solvothermal route. $LiMnPO_4$ prepared by the above mentioned rousted displayed a monotonous charge-discharge curve and exhibited a discharge capacity of ≈15 to 45 mA·h^{-1}. Ji *et al*. [47] also followed a similar approach to yield $LiMnPO_4$ nanostructures using citric acid and sodium dodecyl benzene sulfonate (SDBS) as an additive to tune the morphology of the final product. Also reported the kinetic behavior during Mg_{2+} substitution on Mn site compounds were prepared by a hydrothermal reaction and consequently ball milled carbon (20 wt%) before making electrodes. Increasing the concentration of Mg_{2+} ($LiMn_{1-x}Mg_xPO_4$, x = 0 ≤ 5) provides substantial improvement in the thermal stability of the phase. Ni and Gao [48] reported the synthesis of Cu_{2+} substituted $LiMnPO_4$ by an ascorbic acid mediated synthesis. The obtained particles (≈100 nm) were carbon coated by carbonization of sucrose at 600˚C and carbon content of 2.4 wt% was obtained in the final product. In the range of 2.2 - 4.5 V (CC-CV mode), test cells delivered a reversible capacity of 101, 121 and 76 mA·h·g^{-1} for $LiMnPO_4$, $LiMn_{0.98}Cu_{0.02}PO_4$ and $LiMn_{0.95}Cu_{0.98}PO_4$ phases, respectively. Wang *et al*. [49] reported the solvothermal synthesis of $LiMnPO_4$ nanoplates and rods using sodium dodecyl benzene sulfonate (SDBS). The synthesized powders were carbon coated through chemical vapor deposition (CVD) using methylbenzene as the carbon source and argon as the carrier gas. The authors compared the carbon coating technique with the conventional high energy ball milling (BM) procedure.

The discharge capacities of plate-CVD, Rod-CVD, Plate-BM and Rod-BM were 147, 126, 120 and 92 mA·h·g^{-1}, respectively, between 2.5 and 4.9 V at 0.05C at room temperature by CC mode. Recently, Dokko *et al*. [50] suggested the synthesis of $LiMnPO_4$ nanoparticles by reacting Li_3PO_4 (solid) with molten aqua-complexes of $MnSO_4$ under hydrothermal conditions at 190˚C. Later, the obtained $LiMnPO_4$ particles were carbon coated using sucrose with subsequent heat treatment at 700˚C. The molar ratio of Mn_x and H_2O in the reactor was varied by adding water to the reaction mixture. When x = 7.8, 50 nm size $LiMnPO_4$ particles were obtained which delivered a discharge capacity of ≈135 mA·h·g^{-1} at 0.1 C between 2 and 4.5 V by CC-CV mode.

2.5. Sol-Gel Synthesis

Sol-gel synthesis is a low temperature, wet chemical approach, which is often used for the preparation of metal oxides or other specific compositions. Standard sol-gel synthesis involves the formation of a sol, *i.e.* a stable colloidal suspension of solid particles in a solvent, and the gelation of the sol to form a gel consisting of interconnected rigid skeleton with pores made o colloidal particles. The properties of the gel are determined by the particle size and cross-linking ratio. The gel can then be dried to form xerogel, which shows reduced volume [51]-[54].

To obtain the final powder products, all liquids need to be removed from the surfaces of pores by a heat

treatment carried out at elevated temperatures, which also reduces the number and connectivity of pores, known as densification [53] [54]. Reaction parameters such as temperature, time, pH, precursor, solvent, concentration and viscosity, etc., are of importance for the formation and ultimate morphology (particle size and shape, pore size, and porosity) of the obtained powders. In sol-gel synthesis, the surfaces of the powder products are controlled from the beginning of the reactions. In addition, sol-gel synthesis is low cost and does not require high processing temperature, and powders produced by this method have the advantages or precise stoichiometry control, high purity, uniform structure and very small size. **Table 5** shows the precursors used in the sol-gel method of the resultant $LiMnPO_4$ and composites of this phase. Ethylene glycol assisted synthesis of $LiMnPO_4$ (M = Fe, Mn and Co) nanostructures was reported by Yang and Xu [55] to enable in situ carbon coating. In situ carbon coating over $LiMnPO_4$ particles by using organic precursors was successful and it was found that 3.3 wt% of carbon was covered on the surface after the phase formation at 700˚C in a N_2 atmosphere. The Li/$LiMnPO_4$ cell was cycled between 2.5 and 4.5 V in CC mode and delivered a reversible capacity of 85 and 42 mA·g^{-1} at 0.01 and 0.05 C rates, respectively. Kwon *et al*. [56] successfully synthesized nanosized (140 - 130 nm) $LiMnPO_4$ particles by a glycolic acid assisted sol-gel approach.

The prepared $LiMnPO_4$ was ball milled with 20 wt% carbon size reduction as well as to enable carbon coating. The cycling profiles indicate reduction of particle size from 830 to 140 nm which resulted in improved electrochemical performance ($\approx$134 mA·h·g^{-1} for 140 nm particles) between 2.3 and 4.5 V at 0.1 C. At 1 C, 140 nm particles exhibited a reversible capacity of $\approx$81 mA·h·g^{-1}, whereas 270 nm particles showed a reversible capacity of $\approx$5 mA·h·g^{-1}. A liquid phase synthesis was also reported by Doi *et al*. [57] to reduce the particle size in the presence of long chain oleic acids comprising 18 atoms of carbon. For this synthesis, the total reaction was completed at less than 300˚C resulting in the formation of $LiMnPO_4$. The obtained compound delivered a discharge capacity of 6 mA·h·g^{-1} between 3 and 4.5 V at 0.01C by CC mode. After heat treatment at 500˚C for 1 h in Ar, the long chain oleic acid was burned and converted to carbon. Isovalent and aliovalent doping (Mg_{2+}, Fe_{2+}, Co_{2+}, V_{3+} and Gd_{3+}) on Mn_{2+} sited reported by Yang *et al*. [58] and such phases were prepared by solution phase reaction using citric acid as the carbon source. The precursors were ball-milled for 10 h in a planetary ball miller and fired at 700˚C for 20 h in a N_2 atmosphere. The substitution in Mn sites ($LiMn_{0.95}M_{0.95}PO_4$, M = Mg, V, Fe, Co and Gd) clearly revealed the increase in unit cell volume for all cases, except for Fe_{2+}. The cell delivered a discharge capacity of 45, 61, 32, 102 and 59 mA·h·g^{-1} at room temperature (25˚C), and 113, 120, 95, 149, and 117 mA·h·g^{-1} at an elevated temperature (50˚C) for Mg, V, Fe, Co, and Gd substitutions, respectively, between 2.7 and 4.4 V in CC-CV mode. Preparation of $LiMnPO_4$ composites was suggested by Herrera *et al*. [59].

The authors intended to increase the surface area, thereby achieving full performance of the material by utilizing a conventional coating technique. It is worth mentioning that addition of glucose. This indicates that the presence of carbon coating during the formation of crystallites increases the number of nucleation sited and

Table 5. Precursors used in the sol-gel method of the resultant powders.

Li Precursor	Mn Precursor	PO$_4$ Precursor	Metal Dopant	Carbon Source	Product	Discharge Capacity (mA·h/g)	Ref.
Li(COOCH$_3$)·2H$_2$O	Mn(CH$_3$COO)$_2$·4H$_2$O	H$_3$PO$_4$			LiMnPO$_4$	42 - 85	[55]
LiOH	Mn(CH$_3$COO)$_2$·4H$_2$O	H$_3$PO$_4$			LiMnPO$_4$	5 - 81 - 134	[56]
Li(COOCH$_3$)·2H$_2$O	MnSO$_4$·H$_2$O	NH$_4$H$_2$PO$_4$			LiMnPO$_4$		[57]
Li(COOCH$_3$)·2H$_2$O	Mn(CH$_3$COO)$_2$·4H$_2$O	NH$_4$H$_2$PO$_4$	Mg(NO$_3$)$_2$ V$_2$O$_5$ Co(CH3COO)$_2$ FeCO$_4$ Gd$_2$O$_3$		LiMn$_{0.95}$M$_{0.95}$PO$_4$, M = Mg, V, Fe, Co and Gd* respectively	45, 61, 32, 10, 59 (at 25˚)* and 113, 120, 95, 149, 117 (at 50˚)*	[58]
LiOH	Mn(CH$_3$COO)$_2$·4H$_2$O	H$_3$PO$_4$		Glucose	LiMnPO$_4$/C		[59]
LiNO$_3$	Mn(NO$_3$)$_2$	H$_3$PO$_4$		SWNT	LiMnPO$_4$/SWCN	70	[58]
Li(COOCH$_3$)·2H$_2$O	Mn(CH$_3$COO)$_2$·4H$_2$O	NH$_4$H$_2$PO$_4$		SWNT	LiMnPO$_4$/SWCN	140	[58]
Li(COOCH$_3$)·2H$_2$O	MnSO$_4$·H$_2$O	NH$_4$H$_2$PO$_4$	Co(CH$_3$COO)$_2$		LiMn$_{0.91}$Co$_{0.09}$PO$_4$	148	[58]

leads to increases in the size of the particle. Nithya *et al.* [60] reported synthesis of $LiMn_{0.91}Co_{0.09}PO_4$ by a glycine assisted sol-gel approach with the particle size ranging from 50 to 300 nm. The resultant phase was ball milled with the desired amount of carbon (acetylene black 30 wt%) to yield a high performance cathode. $LiCo_{0.09}Mn_{0.91}PO_4/C$ delivered a maximum discharge capacity of 162 $mA \cdot h \cdot g^{-1}$ between 3 and 4.9 V vs Li (CC mode) at 0.1 C when compared to 70, 140 and 148 $mA \cdot h \cdot g^{-1}$ for $LiMnPO_4$, $LiMnPO_4$ and $LiCo_{0.09}Mn_{0.91}PO_4$ respectively.

As a final remark, it can be observed that the highest Discharge Capacity is reported for $LiMnPO_4/C$ (165 mAh/g, **Table 2**) synthesized by spry pyrolysis, the same composite synthesized by hydrothermal or solvothermal (147 mAh/g, **Table 4**) and by solid state reaction (144 mAh/g, **Table 1**). High values are also reported for $LiMn_{0.5}Fe_{0.5}PO_4$ (155 mAh/g, **Table 1**) by solid state reaction, $LiMn_{0.85}Fe_{0.15}PO_4$ (140 mAh/g, **Table 3**) by chemical co-precipitation, and $LiMn_{0.95}M_{0.95}PO_4$, (M = Co) (149 mAh/g, **Table 5**) by sol-gel method.

These results suggest that those synthesis methods that allow a better control of particle size and morphology can offer a better potential to improve the Discharge Capacity. Another path can be combined Mn with Fe and Co. It also can be observed that the highest Discharge Capacity can be reached for the $LiMnPO_4/C$, and then the addition of Carbon source is also a topic that deserves attentions.

Other phosphates compounds can be used as cathodes in lithium ion batteries. $LiCoPO_4$ (100 $mA \cdot h \cdot g^{-1}$) [61] [62] has higher open circuit voltages, but lower dielectric capacity than those of $LiMnPO_4$. In addition, $Co_2P_4O_7$ has been observed to be formed in delithiated $LiCoPO_4$ electrode, which degrades the lifetime and can be a safety concern as oxygen is involved during the decomposition reaction. Mixtures of phosphates, including $LiCoPO_4$ or $LiFePO_4$ (170 $mA \cdot h \cdot g^{-1}$) [63], with $LiMnPO_4$, have been used for cathode materials. In such mixtures, the operating voltage increases with increasing manganese content [64] [65], while capacity increases with increasing iron content [1]. Although $LiNiPO_4$ also forms the olivine structure [1] it is no typically used as a cathode material. However, nickel has been added to other phosphate cathode materials. Not considering Olivine Phosphate, few examples can be mentioned that can be considered potentially useful: $LiCoO_2$ (140 $mA \cdot h \cdot g^{-1}$), $Li_xMn_2O_4$ (125 $mA \cdot h \cdot g^{-1}$) and nanostructured Vanadium Oxide (VO_x) with Lithium intercalation capacities [66]. It must be mentioned that VO_x can go through structural breakdown during redox cycles. In this scenery, $LiMnPO_4$ can be considered as a promising material for battery cathode.

3. Conclusions

$LiMnPO_4$ have been reviewed focusing mainly on the synthesis method and how to improve the electrochemical properties performance for batteries cathode. For $LiMnPO_4$ small particle size well-shaped crystals are important for enhancing the properties. In particles with a small diameter, the Li ions may diffuse over shorter distances between the surfaces and center during Li intercalation and de-intercalation contributing to the charge/discharge reaction. The variety of synthesis methods offers more possibilities to control desirable structures and high electrochemical performance. However, it is often challenging to obtain all the desired properties.

Typically, solid state methods are of importance in terms of obtaining ordered crystal structure, but they require higher treatment temperature and longer process time, which may lead to larger particle size and lower electrochemical capacity. On the other hand, sol-gel method gives high purity, small particle size, uniform size distribution, and hence relatively higher electrochemical capacity, but additional solvent cost and environment issues are major disadvantages of these methods. Many solid-state and solution-based methods are good candidates for the mass production of $LiMnPO_4$ powders at industrial scale; however the cost, productivity, reproducibility and complexity of these methods must be taken into consideration.

Acknowledgements

References

[1] Padhi, A.K., Nanjundaswamy, K.S. and Goodenough, J.B. (1997) Phospho-Olivines as Positive-Electrode Materials for Rechargeable Lithium Batteries. *Journal of the Electrochemical Society*, **144**, 1188-1194.
http://dx.doi.org/10.1149/1.1837571

[2] Huang, H., Yin, S.-C. and Nazar, L.F. (2001) Approaching Theoretical Capacity of $LiFePO_4$ at Room Temperature at

High Rates. *Electrochemical and Solid-State Letters*, **4**, A170-A172. http://dx.doi.org/10.1149/1.1396695

[3] Bramnik, N.N. and Ehrenberg, H. (2008) Precursor-Based Synthesis and Electrochemical Performance of $LiMnPO_4$. *Journal of Alloys and Compounds*, **464**, 259-264.

[4] Li, G., Azuma, H. and Tohda, M. (2002) $LiMnPO_4$ as the Cathode for Lithium Batteries. *Electrochemical and Solid-State Letters*, **5**, A135-A137. http://dx.doi.org/10.1149/1.1475195

[5] Delacourt, C., Poizot, P., Morcrette, M., Tarascon, J.-M. and Masquelier, C. (2004) One-Step Low-Temperature Route for the Preparation of Electrochemically Active LiMnPO4 Powders. *Chemistry of Materials*, **16**, 93-99.

[6] Arcon, D., Zorko, A., Cevc, P., Dominko, R., Bele, M., Jamnik, J., Jaglicic, Z. and Golosovsky, I. (2004) Weak ferromagnetism of $LiMnPO_4$. *Journal of Physics and Chemistry of Solids*, **65**, 1773-1777.

[7] Santoro, R.P., Segal, D.J. and Newman, R.E. (1966) Magnetic Properties of $LiCoPO_4$ and $LiNiPO_4$. *Journal of Physics and Chemistry of Solids*, **27**, 1192-1193. http://dx.doi.org/10.1016/0022-3697(66)90097-7

[8] Mays, J.M. (1963) Nuclear Magnetic Resonances and Mn-O-P-O-Mn Superexchange Linkages in Paramagnetic and Antiferromagnetic $LiMnPO_4$. *Physical Review Letters*, **131**, 38. http://dx.doi.org/10.1103/PhysRev.131.38

[9] Goni, A., Lezama, L., Barberies, G.E., Pizzaro, J.L., Arriortua, M.I. and Rojo, T. (1996) Magnetic Properties of the $LiMPO_4$ (M = Co, Ni) Compounds. *Journal of Magnetism and Magnetic Materials*, **164**, 251-255. http://dx.doi.org/10.1016/S0304-8853(96)00394-0

[10] Zaspel, C.E., Grigereit, T.E. and Drumheller, J.E. (1995) Soliton Contribution to the Electron Paramagnetic Resonance Linewidth in the Two-Dimensional Antiferromagnetic. *Physical Review Letters*, **74**, 544-765.

[11] Martha, S.K., Grinblat, J., Haik, O., Zinigrad, E., Drezen, T., Miners, J.H., Exnar, I., Kay, A., Markovsky, B. and Aurbach, D. (2009) $LiMn_{0.8}Fe_{0.2}PO_4$: An Advanced Cathode Material for Rechargeable Lithium Batteries. *Angewandte Chemie International Edition*, **48**, 8559-8563. http://dx.doi.org/10.1002/anie.200903587

[12] Son, C.G., Yang, H.M., Lee, G.W., Cho, A.R., Aravindan, V., Kim, H.S., Kim, W.S. and Lee, Y.S.J. (2011) Manipulation of Adipic Acid Application on the Electrochemical Properties of $LiFePO_4$ at High Rate Performance. *Journal of Alloys and Compounds*, **509**, 1279-1284. http://dx.doi.org/10.1016/j.jallcom.2010.10.009

[13] Kang, B. and Ceder, G. (2010) Electrochemical Performance of $LiMnPO_4$ Synthesized with Off-Stoichiometry. *Journal of the Electrochemical Society*, **157**, A808-A811. http://dx.doi.org/10.1149/1.3428454

[14] Hu, C.L., Yi, H.H., Fang, H.S., Yang, B., Yao, Y.C., Ma, W.H. and Dai, Y.N. (2010) Improving the Electrochemical Activity of LiMnPO4 via Mn-Site Co-Substitution with Fe and Mg. *Electrochemistry Communications*, **12**, 1784-1787. http://dx.doi.org/10.1016/j.elecom.2010.10.024

[15] Yi, H., Hu, C., Fang, H., Yang, B., Yao, Y., Ma, W. and Dai, Y. (2011) Optimized Electrochemical Performance of $LiMn_{0.9}Fe_{0.1-x}Mg_xPO_4/C$ for Lithium Ion Batteries. *Electrochimica Acta*, **56**, 4052-4057. http://dx.doi.org/10.1016/j.electacta.2011.01.121

[16] Hong, J., Wang, F., Wang, X. and Graetz, J. (2011) $LiFe_xMn_{1-x}PO_4$: A Cathode for Lithium-Ion Batteries. *Journal of Power Sources*, **196**, 3659-3663. http://dx.doi.org/10.1016/j.jpowsour.2010.12.045

[17] Muraliganth, T. and Manthiram, A. (2010) $LiM_{1-y}M_yPO_4$ (M = Fe, Mn, Co, and Mg) Solid Solution Cathodes. *Journal of Physical Chemistry C*, **114**, 15530-15540. http://dx.doi.org/10.1021/jp1055107

[18] Lee, S.J. (2002) Materials Science and Engineering. Ph.D. Thesis, Kyungnam University, Changwon.

[19] Lee, J.H., Jung, K.Y. and Park, S.B. (1999) Modification of Titania Particles by Ultrasonic Spray Pyrolysis of Colloid. *Journal of Materials Science*, **34**, 4089-4093.

[20] Teng, T.H., Yang, M.-R., Wu, S.H. and Chiang, Y.P. (2007) Electrochemical Properties of $LiFe_{0.9}Mg_{0.1}PO_4/Carbon$ Cathode Materials Prepared by Ultrasonic Spray Pyrolysis. *Solid State Communications*, **142**, 389-392.

[21] Bakenov, Z. and Taniguchi, I. (2010) Electrochemical Performance of Nanocomposite $LiMnPO_4/C$ Cathode Materials for Lithium Batteries. *Electrochemistry Communications*, **12**, 75-78. http://dx.doi.org/10.1016/j.elecom.2009.10.039

[22] Bakenov, Z. and Taniguchi, I. (2010) Physical and Electrochemical Properties of $LiMnPO_4/C$ Composite Cathode Prepared with Different Conductive Carbons. *Journal of Power Sources*, **195**, 7445-7451. http://dx.doi.org/10.1016/j.jpowsour.2010.05.023

[23] Bakenov, Z. and Taniguchi, I. (2011) Synthesis of Spherical $LiMnPO_4/C$ Composite Microparticles. *Materials Research Bulletin*, **46**, 1311-1314. http://dx.doi.org/10.1016/j.materresbull.2011.03.020

[24] Doan, T.N.L., Bakenov, Z. and Taniguchi, I. (2010) Preparation of Carbon Coated $LiMnPO_4$ Powders by a Combination of Spray Pyrolysis with Dry Ball-Milling Followed by Heat Treatment. *Advanced Powder Technology*, **21**, 187-196. http://dx.doi.org/10.1016/j.apt.2009.10.016

[25] Doan, T.N.L. and Taniguchi, I. (2011) Cathode Performance of $LiMnPO_4/C$ Nanocomposites Prepared by a Combination of Spray Pyrolysis and Wet Ball-Milling Followed by Heat Treatment. *Journal of Power Sources*, **196**, 1399-1408. http://dx.doi.org/10.1016/j.jpowsour.2010.08.067

[26] Taniguchi, I., Doan, T.N.L. and Shao, B. (2011) Synthesis and Electrochemical Characterization of LiCo$_x$Mn$_{1-x}$PO$_4$/C Nanocomposites. *Electrochimica Acta*, **56**, 7680-7685. http://dx.doi.org/10.1016/j.electacta.2011.06.055

[27] Oh, S.M., Jung, H.G., Yoon, C.S., Myung, S.T., Chen, Z., Amine, K. and Sun, Y.K. (2011) Enhanced Electrochemical Performance of Carbon-LiMn$_{1-x}$Fe$_x$PO$_4$ Nanocomposite Cathode for Lithium-Ion Batteries. *Journal of Power Sources*, **196**, 6924-6928. http://dx.doi.org/10.1016/j.jpowsour.2010.11.159

[28] Oh, S.M., Oh, S.W., Myung, S.T., Lee, S.M. and Sun, Y.K. (2010) The Effects of Calcination Temperature on the Electrochemical Performance of LiMnPO$_4$ Prepared by Ultrasonic Spray Pyrolysis. *Journal of Alloys and Compounds*, **506**, 372-376. http://dx.doi.org/10.1016/j.jallcom.2010.07.010

[29] Oh, S.M., Oh, S.W., Yoon, C.S., Scrosati, B., Amine, K. and Sun, Y.K. (2010) High-Performance Carbon-LiMnPO$_4$ Nanocomposite Cathode for Lithium Batteries. *Advanced Functional Materials*, **20**, 3260-3265. http://dx.doi.org/10.1002/adfm.201000469

[30] Xiao, J., Chernova, N.A., Upreti, S., Chen, X., Li, Z., Deng, Z., Choi, D., Xu, W., Nie, Z., Graff, G.L., Liu, J., Whittingham, M.S. and Zhang, J.-G. (2011) Electrochemical Performances of LiMnPO$_4$ Synthesized from Non-Stoichiometric Li/Mn Ratio. *Physical Chemistry Chemical Physics*, **13**, 18099-18106. http://dx.doi.org/10.1039/c1cp22658d

[31] Kim, D.-K., Park, H.-M., Jung, S.-J., Jeong, Y.U., Lee, J.-H. and Kim, J.-J. (2006) Effect of Synthesis Conditions on the Properties of LiFePO$_4$ for Secondary Lithium Batteries. *Journal of Power Sources*, **159**, 237-240. http://dx.doi.org/10.1016/j.jpowsour.2006.04.086

[32] Oh, S.-M., Myung, S.-T., Choi, Y.S., Oh, K.H. and Sun, Y.-K. (2011) Co-Precipitation Synthesis of Micro-Sized Spherical LiMn$_{0.5}$Fe$_{0.5}$PO$_4$ Cathode Material for Lithium Batteries. *Journal of Materials Chemistry*, **21**, 19368-19374. http://dx.doi.org/10.1039/c1jm13889h

[33] Sun, Y.-K., Oh, S.-M., Park, H.-K. and Scrosati, B. (2011) Micrometer-Sized, Nanoporous, High-Volumetric-Capacity LiMn$_{0.85}$Fe$_{0.15}$PO$_4$ Cathode Material for Rechargeable Lithium-Ion Batteries. *Advanced Materials*, **23**, 5050-5054. http://dx.doi.org/10.1002/adma.201102497

[34] Oh, S.-M., Myung, S.-T., Park, J.B., Scrosati, B., Amine, K. and Sun, Y.-K. (2012) Double-Structured LiMn$_{0.85}$Fe$_{0.15}$PO$_4$ Coordinated with LiFePO$_4$ for Rechargeable Lithium Batteries. *Angewandte Chemie International Edition*, **51**, 1853-1856. http://dx.doi.org/10.1002/anie.201107394

[35] Wold, A. and Dwight, K. (1993) Solid State Chemistry: Synthesis, Structure, and Properties of Selected Oxides and Sulfides. Chapman & Hall Incorporation, New York. http://dx.doi.org/10.1007/978-94-011-1476-9

[36] Avvakumov, E.G., Senna, M. and Kosova, N. (2001) Soft Mechanochemical Synthesis: A Basis for New Chemical Technologies. Kluwer Academic Publishers, New York.

[37] Sōmiya, S. and Roy, R. (2000) Hydrothermal Synthesis of Fine Oxide Powders. *Bulletin of Materials Science*, **23**, 453-460.

[38] Fang, H., Li, L. and Li, G. (2007) Hydrothermal Synthesis of Electrochemically Active LiMnPO$_4$. *Chemistry Letters*, **36**, 436-437. http://dx.doi.org/10.1246/cl.2007.436

[39] Fang, H., Li, L., Yang, Y., Yan, G. and Li, G. (2008) Carbonate Anions Controlled Morphological Evolution of LiMnPO$_4$ Crystals. *Chemistry Letters*, **2008**, 1118-1120. http://dx.doi.org/10.1039/b716916g

[40] Chen, G., Wilcox, J.D. and Richardson, T.J. (2008) Improving the Performance of Lithium Manganese Phosphate through Divalent Cation Substitution. *Electrochemical and Solid-State Letters*, **11**, A190-A194. http://dx.doi.org/10.1149/1.2971169

[41] Wang, Y., Yang, Y. and Shao, H. (2009) Fabrication of Microspherical LiMnPO$_4$ Cathode Material by a Facile One-Step Solvothermal Process. *Materials Research Bulletin*, **44**, 2139-2142. http://dx.doi.org/10.1016/j.materresbull.2009.06.019

[42] Wang, Y., Yang, Y. and Shao, H. (2010) Enhanced Electrochemical Performance of Unique Morphological Cathode Material Prepared by Solvothermal Method. *Solid State Communications*, **150**, 81-85. http://dx.doi.org/10.1016/j.ssc.2009.09.046

[43] Saravanan, K., Vittal, J.J., Reddy, M.V., Chowdari, B.V.R. and Balaya, P. (2010) Storage Performance of LiFe$_{1-x}$MnxPO$_4$ Nanoplates (*x* = 0, 0.5, and 1). *Journal of Solid State Electrochemistry*, **14**, 1755-1760. http://dx.doi.org/10.1007/s10008-010-1031-y

[44] Manthiram, A., Vadivel Murugan, A., Sarkar, A. and Muraliganth, T. (2008) Nanostructured Electrode Materials for Electrochemical Energy Storage and Conversion. *Energy & Environmental Science*, **1**, 621-638. http://dx.doi.org/10.1039/b811802g

[45] Vadivel Murugan, A., Muraliganth, T., Ferreira, P.J. and Manthiram, A. (2009) Dimensionally Modulated, Single-Crystalline LiMPO$_4$ (M= Mn, Fe, Co, and Ni) with Nano-Thumblike Shapes for High-Power Energy Storage. *Inorganic Chemistry*, **48**, 946-952. http://dx.doi.org/10.1021/ic8015723

[46] Vadivel Murugan, A., Muraliganth, T. and Manthiram, A. (2009) One-Pot Microwave-Hydrothermal Synthesis and Characterization of Carbon-Coated LiMPO$_4$ (M = Mn, Fe, and Co) Cathodes. *Journal of the Electrochemical Society*, **156**, A79-A83. http://dx.doi.org/10.1149/1.3028304

[47] Ji, H., Yang, G., Ni, H., Roy, S., Pinto, J. and Jiang, X. (2011) General Synthesis and Morphology Control of LiMnPO$_4$ Nanocrystals via Microwave-Hydrothermal Route. *Electrochimica Acta*, **56**, 3093-3100. http://dx.doi.org/10.1016/j.electacta.2011.01.079

[48] Ni, J. and Gao, L. (2011) Effect of Copper Doping on LiMnPO$_4$ Prepared via Hydrothermal Route. *Journal of Power Sources*, **196**, 6498-6501. http://dx.doi.org/10.1016/j.jpowsour.2011.03.073

[49] Wang, F., Yang, J., Gao, P., NuLi, Y. and Wang, J. (2011) Morphology Regulation and Carbon Coating of LiMnPO$_4$ Cathode Material for Enhanced Electrochemical Performance. *Journal of Power Sources*, **196**, 10258-10262. http://dx.doi.org/10.1016/j.jpowsour.2011.08.090

[50] Dokko, K., Hachida, T. and Watanabe, M.J. (2011) LiMnPO$_4$ Nanoparticles Prepared through the Reaction between Li$_3$PO$_4$ and Molten Aqua-Complex of MnSO$_4$. *Journal of the Electrochemical Society*, **158**, A1275-A1281. http://dx.doi.org/10.1149/2.015112jes

[51] Sangeeta, D. and LaGraff, J.R. (2005) Inorganic Materials Chemistry Desk Reference. 2nd Edition, CRC Press, Boca Raton.

[52] Bergna, H.E. and Roberts, W.O. (2006) Colloidal Silica: Fundamentals and Applications. 2nd Edition, CRC Press, Boca Raton.

[53] Brinker, C.J. and Scherer, G.W. (1990) Solgel Science: The Physics and Chemistry of Solgel Processing. Academic Press Incorporation, San Diego.

[54] Hench, L.L. and West, J.K. (1990) The Sol-Gel Process. *Chemical Reviews*, **90**, 33-72.

[55] Yang, J. and Xu, J.J. (2006) Synthesis and Characterization of Carbon-Coated Lithium Transition Metal Phosphates LiMPO$_4$ (M = Fe, Mn, Co, Ni) Prepared via a Nonaqueous Sol-Gel Route. *Journal of Power Sources*, **153**, A716-A723. http://dx.doi.org/10.1149/1.2168410

[56] Kwon, N.H., Drezen, T., Exnar, I., Teerlinck, I., Isono, M. and Graetzel, M. (2006) Enhanced Electrochemical Performance of Mesoparticulate LiMnPO$_4$ for Lithium Ion Batteries. *Electrochemical and Solid-State Letters*, **9**, A277-A280. http://dx.doi.org/10.1149/1.2191432

[57] Doi, T., Yatomi, S., Kida, T., Okada, S. and Yamaki, J.I. (2011) Liquid-Phase Synthesis of Uniformly Nanosized LiMnPO$_4$ Particles and Their Electrochemical Properties for Lithium-Ion Batteries. *Crystal Growth & Design*, **9**, 4990-4992.

[58] Yang, G., Ni, H., Liu, H., Gao, P., Ji, H., Roy, S., Pinto, J. and Jiang, X. (2011) The Doping Effect on the Crystal Structure and Electrochemical Properties of LiMn$_x$M$_{1-x}$PO$_4$ (M=Mg, V, Fe, Co, Gd). *Journal of Power Sources*, **196**, 4747-4755.

[59] Herrera, J., Fuentes, L., Diaz, S., Camacho, H., Trinidad, J. and Alvarez, L. (2014) Synthesis and Structural Characterization of Manganese Olivine Lithium Phosphate. *Journal Alloys and Compounds*, in press.

[60] Nithya, C., Thirunakaran, R., Sivashanmugam, A. and Gopukumar, S. (2012) LiCo$_x$Mn$_{1-x}$PO$_4$/C: A High Performing Nanocomposite Cathode Material for Lithium Rechargeable Batteries. *Chemistry—An Asian Journal*, **7**, 163-168. http://dx.doi.org/10.1002/asia.201100485

[61] Murugan, A.V., Muraliganth, T. and Manthiram, A. (2009) One-pot Microwave-Hydrothermal Synthesis and Characterization of Carbon-Coated LiMPO$_4$ (M= Mn, Fe, and Co) Cathodes. *Journal of the Electrochemical Society*, **156**, A79-A83. http://dx.doi.org/10.1149/1.3028304

[62] Bramnik, N.N., Nikolowski, K., Trots, D.M. and Ehrenberg, H. (2008) Thermal Stability of LiCoPO4 Cathodes. *Electrochemical and Solid-State Letters*, **11**, A89-A93. http://dx.doi.org/10.1149/1.2894902

[63] Whittingham, M.S. (2004) Lithium Batteries and Cathode Materials. *Chemical Reviews*, **104**, 4271-4301. http://dx.doi.org/10.1021/cr020731c

[64] Baek, D.-H., Kim, J.-K., Shin, Y.-J., Chauhan, G.S., Ahn, J.-H. and Kim, K.-W. (2009) Effect of Firing Temperature on the Electrochemical Performance of LiMn0.4Fe0.6PO4/C Materials Prepared by Mechanical Activation. *Journal of Power Sources*, **189**, 59-65. http://dx.doi.org/10.1016/j.jpowsour.2008.11.051

[65] Kobayashi, G., Yamada, A., Nishimura, S.-I., Kanno, R., Kobayashi, Y., Seki, S., Ohno, Y. and Miyashiro, H. (2009) Shift of Redox Potential and Kinetics in Lix(Mn$_y$Fe$_{1-y}$)PO4. *Journal of Power Sources*, **189**, 397-401. http://dx.doi.org/10.1016/j.jpowsour.2008.07.085

[66] Wang, Y. and Cao. G. (2008) Developments in Nanostructured Cathode Materials for High-Performance Lithium-Ion Batteries. *Advanced Materials*, **20**, 2251-2269. http://dx.doi.org/10.1002/adma.200702242